Improving the geometry of a 3D longitudinal network using a stretched wire

Stéphane Durand, Thomas Touze, Vivien Rude, Helene Mainaud Durand

IMPROVING THE GEOMETRY OF A 3D LONGITUDINAL NETWORK USING A STRETCHED WIRE

S. Durand, (GeF, Le Mans, France), T. Touzé, (Heig-VD, Yverdon, Switzerland)
V. Rude, H. Mainaud-Durand, (CERN, Geneva, Switzerland)

Abstract

In this paper, we show that integrating a common stretched wire in a 3D longitudinal network improve the geometry of the geodetic network, both in terms of accuracy and reliability. We used a polypropolen braided rope type, lightly tensed wire with a sag value of the order of half a meter. In our 3D longitudinal test network, angle and distances measurements carried out between points using a total station formed the basic network. In addition, vertical and horizontal angle measurements were performed on marks located on the wire to densify the network. In the first part of this contribution, we detail the functional models developed to take into account points on the wire. We also describe a test campaign carried out with a wire stretched over 50 m, within a 5 m wide and 60 m long network. In the second part, we present and discuss our results, and show that using a stretched wire can improve significantly the accuracy and reliability of the network points determination.

INTRODUCTION

The alignment of the components of a particle accelerator is a challenging task as the accuracy requirements can be very small (up to a few tens of micrometers) in a straight and narrow tunnel. In such a particular geometry configuration, it is difficult to obtain the required accuracy with standard 3D measurements.

Since 50 years, surveyors have been developing various specific tools and methods to align the elements of the machines more efficiently and more accuratly than with standard 3D measurements. One of these tool is the stretched wire, which provides a straight line over a distance of up to several hundred meters at least radially. In vertical, one has to take into account the catenary shape of the wire. This solution has the advantage to be insensitive to lateral refraction whose is not negligeable in tunnels. At Cern, stretched wires are used since more than 50 years [1] jointly with ecartometers or Wire Positioning Systems [2], [3]. In the LHC machine for example, stretched wires combined with ecartometers are used to achieve an alignment accuracy of the order of 0.1 mm at 1-sigma confidence level, over sliding windows of 150 m.

Currently, CERN uses WPS sensors to perform the micrometric position monotoring of specific quadrupoles located before the four collision points of the LHC. The sensors carry out offset measurements with respect to a carbon PEEK wire (350μm diameter, mass per unit length of about 0.000235 kg/m, tension force of 150 N). In these conditions, the shape of the stretched wire is close to a second order polynomial for distances below 500m [4] and can be modeled in the vertical plane knowing the difference of height of at least three points along the wire.

In [5], the authors showed that in a 3D longitudinal network, determined by standard 3D measurements, typically performed using industrial total station or absolute tracker, the determination of the radial position of the components can be improved by adding straight line constraints for points of the network located onto a stretched wire. In this work, measurements were indirectly performed onto the wire using capacitive WPS sensors: the absolute position of the wire was determined using WPS sensors in its reference frame, and metrological plates equipped with 0.5 inches prims were used to connect WPS measurements and standard 3D measurements.

The main objective of the present contribution is to study the advantages of using a basic stretched wire in a 3D longitudinal network, with measurements directly performed on the wire with a total station. Our work will focus in particular on the improvement in terms of accuracy and reliability. The methodology proposed is the following: a polypropolen braided rope is stretched along a longitudinal network and marked with a pen. Vertical and horizontal angle measurements are performed on the marks located on the wire from a set of points of the network, in addition to the angles and distances measurements performed between points, using a total station. All the measurements carried out in the network are processed together using the least squares method, and both coordinates of the points and parameters of the wire are estimated.

STRETCHED WIRE MECHANICS

If a chain or rope is hanged between two fixed points, namely O and P, it takess a catenary shape (Figure 2). Let B be the lowest point of the chain, and consider $\left(B, e^b, n^b, z^b\right)$ the local astronomical system at point B, with the negative z-axis defined by the gravity vector at B. At first order, the catenary can be considered as included in a vertical plane. Let γ be the azimut of the plane containing the catenary, and h^b the horizontal axis corresponding to the direction with azimut γ. For each point D on the chain, h denotes the horizontal distance between points B and D (i.e. absissa along the h^b axis), s denotes the curvilinear abscissa of point D with an origin at point B. The portion BD

of the chain is in equilibrium under the action of three forces: the horizontal tension T at B, the tension S at D (both in Newtons), which makes an angle θ with the horizontal, and the weight of the portion BD. As indicated in [4], the following relations can be derived from Figures 1 and 2:

$$\frac{dz}{dh} = \tan\theta = \frac{Q}{T} = \frac{gqs}{T} \tag{1}$$

$$ds^2 = dh^2 + dz^2 \tag{2}$$

Where q is the mass per unit length of the chain (kg/m), and g is the standard acceleration due to gravity (m/s^2).

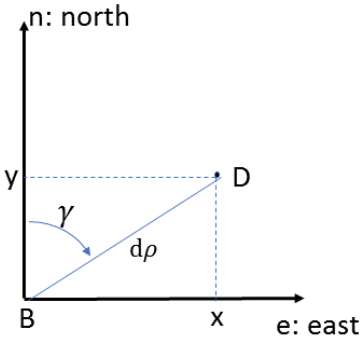

Figure 1: Azimut of the vertical plane containing the stretched wire.

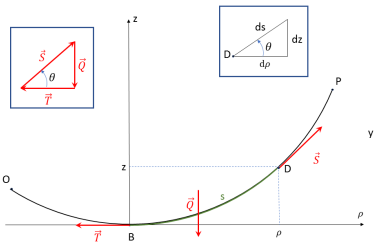

Figure 2: The catenary in the vertical plane containing the stretched wire.

From equations 1 and 2, it is possible to express the curvilinear abscissa as a function of the horizontal distance:

$$s(h) = \alpha \sinh\frac{h}{\alpha} \tag{3}$$

Where $\alpha = \frac{T}{qg}$ is a constant, having the dimensions of length. For wires typically used at CERN, α values are about 65000. From equation 3, and knowing that $z(0) = 0$ at point B, the equation of the catenary is:

$$z(h) = \alpha\left(\cosh\frac{h}{\alpha} - 1\right) \tag{4}$$

Thus, in order to define a stretched wire, five parameters are required: (a) the coordinates of the lowest point B on the wire, (b) the azimut of the vertical plane containing the wire, and (c) the α-constant of the wire.

FUNCTIONAL MODEL

Let's consider a network where conventional measurements (i.e. direction angles, zenith angles and slope distances) are performed using a total station. In this network, a particular point S is performing measurements on a point F. We can express the coordinates of the points S and F in the local astronomical 3D coordinate system of point S: (e_S^s, n_S^s, z_S^s) and (e_F^s, n_F^s, z_F^s) where exponent s indicates that the coordinates are related to the local astronomical system of point S. Direction and zenith angles from point S to point F can be expressed from the local coordinates of points S and F in the local astronomical system at point S as follows:

$$L_{SF} = \arctan\left(\frac{e_F^s - e_S^s}{n_F^s - n_S^s}\right) - G_{0,S} \tag{5}$$

$$A_{SF} = \arctan\left(\frac{\sqrt{(e_F^s - e_S^s)^2 + (n_F^s - n_S^s)^2}}{z_F^s - z_S^s}\right) \tag{6}$$

Where $G_{0,S}$ denotes the orientation unknown for station S.

In order to express these observation equations in terms of Cartesian coordinates in a geodetic Cartesian reference system, denote Φ_S (resp. Λ_S) the astronomical latitude (resp. longitude) of point S. It is then possible to compute matrix R^S such as:

$$\begin{bmatrix} e_F^s - e_B^s \\ n_F^s - n_B^s \\ z_F^s - z_B^s \end{bmatrix} = \begin{bmatrix} R_{11}^S & R_{12}^S & R_{13}^S \\ R_{21}^S & R_{22}^S & R_{23}^S \\ R_{31}^S & R_{32}^S & R_{33}^S \end{bmatrix} \begin{bmatrix} X_F - X_S \\ Y_F - Y_S \\ Z_F - Z_S \end{bmatrix} \tag{7}$$

As some point F may be located onto a stretched wire, we also have to consider the local astronomical system (B, e^b, n^b, z^b) associated with the lowest point of the wire B. We denote (e_P^b, n_P^b, z_P^b) the local coordinates of point P in this coordinate system.

In our processing scheme, our objective is to estimate the coordinates of unknown points in the network, using the fact that some points are located onto a stretched wire. The parameters of these points are the coordinates of the lowest point, the azimuth of the plane containing the wire and the α-constant of the wire. We have chosen to express the observation equations 5 and 6 as functions of the parameters of the stretched wire. Thus, we do not directly estimate the unknown coordinates of points onto the wire. As showed by Figures 1 and 2, for a point F onto the stretched wire, the following relationships exist:

$$e_F^b - e_B^b = h_F . \sin\gamma \tag{8}$$

$$n_F^b - n_B^b = h_F . \cos\gamma \tag{9}$$

$$z_F^b - z_B^b = \alpha \left(\cosh \frac{h_F}{\alpha} - 1 \right) \tag{10}$$

For each point F onto the wire, we thus only estimate parameter h_F as the (e_F^b, n_F^b, z_F^b) coordinates of point F can be expressed as a function of the h_F parameter and of the parameters of the wire.

Using equation 5, we can write:

$$L_{SP} = \arctan \left(\frac{e_F^s - e_B^s + e_B^s - e_S^s}{n_F^s - n_B^s + n_B^s - n_S^s} \right) - G_{0,S} \tag{11}$$

Using the astronomical latitude Φ_S (resp. Φ_B) and longitude Λ_S (resp. Λ_B) of point S (resp. point B), it is possible to compute the rotation matrix R such as:

$$\begin{bmatrix} e_F^s - e_B^s \\ n_F^s - n_B^s \\ z_F^s - z_B^s \end{bmatrix} = \begin{bmatrix} R_{ij} \end{bmatrix} \begin{bmatrix} e_F^b - e_B^b \\ n_F^b - n_B^b \\ z_F^b - z_B^b \end{bmatrix} \tag{12}$$

Thus, equation 5 can be expressed as follows:

$$L_{SP} = \arctan \left(\frac{\Delta e + e_B^s - e_S^s}{\Delta n + n_B^s - n_S^s} \right) - G_{0,S} \tag{13}$$

Following the same method, equation 6 can be expressed as follows:

$$A_{SP} = \arctan \left(\frac{\sqrt{(\Delta e + e_B^s - e_S^s)^2 + (\Delta n + n_B^s - n_S^s)^2}}{\Delta z + z_B^s - z_S^s} \right) \tag{14}$$

Where:

$$\begin{aligned} \Delta e &= R_{11} h_F \sin\gamma + R_{12} h_F \cos\gamma & (15)\\ &\quad + R_{13}\alpha \left(\cosh \frac{h_F}{\alpha} - 1 \right) & (16)\\ \Delta n &= R_{21} h_F \sin\gamma + R_{22} h_F \cos\gamma & (17)\\ &\quad + R_{23}\alpha \left(\cosh \frac{h_F}{\alpha} - 1 \right) & (18)\\ \Delta z &= R_{31} h_F \sin\gamma + R_{32} h_F \cos\gamma & (19)\\ &\quad + R_{33}\alpha \left(\cosh \frac{h_F}{\alpha} - 1 \right) & (20) \end{aligned}$$

Using now rotation matrix R^S, observation equations can be expressed as functions of the cartesian coordinates of points B, S, the parameters of the stretched wire and parameter h_F of point F.

TEST NETWORK

In order to test our methodology, we have conducted several tests in a test network located on the sub-level of the main building of the ESGT engineer school. As shown in Figure 3, the network is approximately 60 m long and 5 m large. A wire has been stretched on approximately 50 m along the longitudinal axis of the network, as illustrated on Figure 4. The network is composed by two points fixed in coordinates (namely P3 and P1), 4 points where total station or reflector can be installed (P1, P2, T5 and P3) and 5 points located on the stretched wire (F1 to F5).

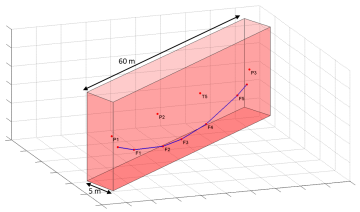

Figure 3: Test network.

The wire used for this campaign is obviously different from the ones used at CERN: it is a polypropolen braided rope, with a diameter of approximately 2 mm, stretched at approximately 1.3 kg, with a mass per unit length of about 0.022 kg/m. In our tests, the sag of the wire is approximately 70 cm, and it is no longer possible to approximate the catenary with a second order polynomial. In our tests, the α-coefficient of the stretched wire has a typical value of about 650.

Figure 4: Left: the stretched wire along the longitudinal axis of our test laboratory. Right: the stretched wire, a 2 mm diameter polypropolen builders line, with marks done with a pen.

All measurements were performed in both telescope faces, using a Leica TM30 total station. Figure 5 summarizes the measurements performed in our test network. Reciprocal measurements were performed

beetween points where a total station could be installed (P1, P2, T5, and P3). As the network is a longitudinal one, and points are nearly on the same line, measurements were performed only to previous and next points. For each point on the wire, measurements were performed on it from at least two other points of the network. We considered a standard deviation of 0.15 mgon for both zenith and direction angles, and of $\pm 0.5\text{mm} \pm 0.5ppm$ for slope distances. Distances were corrected for systematic errors:

- atmospheric EDM errors were corrected following [7] and using the Vaisala meteorological sensors distributed in the test laboratory (one PTB210 pressure sensor, one HMP231 relative humidity sensor and 9 PT100 temperature sensors)
- zero and cyclic errors of EDM instrument/reflector pairs were corrected using calibration values determined with the ESGT calibration bench, a 50 m long bench based on the comparison between EDM and interferometric distance measurements. Such a bench is equipped with a motorized carriage, holding the EDM reflector and interferometric prism, that is moved along the bench.

For all measurements, a centering error of 0.3 mm was considered for both stations and targets (when the target was not on the wire). A centering error of 0.5 mm was considered for operator pointing errors on points located onto the wire.

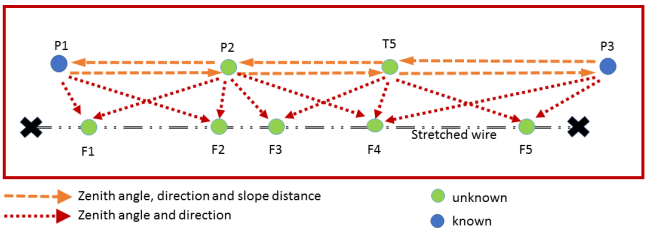

Figure 5: Angles and distances measurements in the test network. Blue dots are points known in 3D coordinates. Green dots are unknown points. Dashed arrows indicate that measurements were performed between points (only angles measurements or angles and distance measurements).

RESULTS AND DISCUSSION

In order to study the impact of using a stretched wire in a longitudinal network, in terms of accuracy and reliability, two processing strategies were used:

- Strategy 1: the network adjustment do not use the fact that some points are located on a stretched wire.
- Strategy 2: the network adjustment takes into account the stretched wire, and makes use of the modified functional models of equations 13 and 14.

Table 1 summarizes relevant informations about the processing strategies. In both strategies, the number of observations (40), of known points (2) and of unknown points (7) are the same. In Strategy 1, which corresponds to a classical adjustment with no wire, we have 21 unknown coordinates (7 unknown points, 3 coordinates per point) and 4 unknown directions, as measurements are performed from points P1, P2, T5 and P3 to the other points of the network. In Strategy 2, we have the same 4 direction parameters than in Strategy 1. For points not located on the wire, we have to estimate their 3D coordinates (P2 and T5), which leads to 6 unknown coordinates. For each point located on the wire, we do not estimate the 3D coordinates but only the h_F parameter. The 3D coordinates are linked to the h_F parameter and to the 5 parameters of the wire. As 5 points (F1 to F5) are located on the wire, we have to estimate 5 h_F parameters plus the 5 parameters of the wire. Therefore, the number of unknowns in Strategy 2 is smaller than in Strategy 1, and as the degree of freedom in Strategy 2 is greater than in Strategy 1, we may expect improvement of the geometry of the network. Table 1 also indicates the estimated variance factors obtained from our data processing. As these values are close to one, we can consider that our measurements are coherent with our functional and stochastic models.

Information	Strategy 1	Strategy 2
Nb. of observations	40	40
Nb. of unknowns (total count)	25	20
Nb. of unknowns (coordinates)	21	6
Nb. of unknowns (due to the wire)	0	10
Degree of freedom	15	20
Estimated variance factor	0.97	0.93

Table 1: Relevant informations about each processing strategy.

The results presented in this contribution were obtained using the CoMeT (Compensation de Mesures Topographiques) application, a network adjustment and design program developped at the GeF laboratory [8]. The functional models related to equations 13 and 14 were implemented in the CoMeT application in order to be able to take into account the use of a stretched wire.

We first compared the estimated standard deviation

along the radial axis for all points, with regards to the degree of freedom of the least squares process. Table 2 shows, for each processing strategy, the estimated standard deviation, at a 95%-confidence level, along the radial axis of the network. It also indicates in parenthesis the percentage of improvement of the estimated standard deviation compared to Strategy 1.

Point	Strategy 1	Strategy 2
P2	0.9	0.7 (17)
T5	0.9	0.8 (18)
F1	1.1	1.0 (8)
F2	1.4	0.8 (42)
F3	1.5	0.8 (47)
F4	1.4	0.8 (44)
F5	1.0	1.0 (3)

Table 2: Estimated standard deviation (at a 95% confidence level) along the radial axis of the network for each processing strategy, in millimeters. In parenthesis, the percentage of improvement over Strategy 1.

In our 3D longitudinal network, where known points are located at the ends of the network, it is expected that the standard deviation along the radial axis is better near the known points and decrease when one moves away from them. This phenomenon corresponds to the obtained standard deviations for Strategy 1 as indicated in Table 2: points F1 and F5, close to points P1 and P3, have standard deviations of about 1 mm. Points F2, F3 and F4, located in the middle of our network, have standard deviations of about 1.5 mm. Table 2 shows that in Strategy 2, for all points, the standard deviation along the radial axis is lower than in Strategy 1: using functional models which include the parameters of the wire really improves the standard deviation. Points F2, F3 and F4, located on the wire, in the middle of our network benefit the most from the improvement (about 47%). Points F1 and F5, located close to the known points P1 and P3 benefit the less from the improvement (respectively 8 and 3 %). Points P2 and T5, not located on the wire, also benefit from the improvement (about 17 %).

Table 3 shows, for each processing strategy, the estimated standard deviation, at a 95%-confidence level, along the longitudinal and vertical axes of the network. For Strategy 2, it also indicates in parenthesis the percentage of improvement of the estimated standard deviation with respect to Strategy 1. Along the longitudinal axis, estimated standard deviations are worst than along the others axes, especially for points located onto the wire. This is mainly due to operator pointing errors when performing measurements on the marks on the wire (we used a centering error of 0.5 mm). Our simulations show that if we are able to improve the pointing accuracy on the wire, the estimated standard deviations along the longitudinal axis will be close to the one along the other axes. Nevertheless Table 3 shows that using Strategy 2 improves the estimated standard deviation along the longitudinal axis, with a percentage of improvement for all points which do no exceed 11 %. Along the vertical axis, Table 3 shows that using Strategy 2 improves the estimated standard deviations, especially for points located on the wire (angles measurements only) and in the middle of the network, with a maximum value of improvement of 38 % for point F3.

Point	Strategy 1		Strategy 2	
	Long.	Vert.	Long.	Vert.
P2	0.7	0.4	0.7 (3)	0.4 (4)
T5	0.7	0.4	0.7 (3)	0.4 (4)
F1	2.8	0.8	2.6 (5)	0.7 (12)
F2	1.9	0.9	1.7 (11)	0.6 (32)
F3	2.9	0.9	2.7 (8)	0.6 (38)
F4	1.8	0.7	1.6 (8)	0.6 (12)
F5	3.9	0.8	3.8 (3)	0.8 (1)

Table 3: Estimated standard deviation (at a 95% confidence level) along the longitudinal and vertical axes of the network for each processing strategy, in millimeters. In parenthesis, the percentage of improvement with respect to Strategy 1.

Figure 6 shows the distribution of the redundancy contribution values for all the observations in each strategy in the commonly used intervals $[0, 0.3[$, $[0.3, 0.60]$ and $]0.6, 1]$ as indicated in [6]. This figure shows that in Strategy 1, 16 observations have a redundancy contribution under the minimum acceptable value for a 3D network against 11 in Strategy 2. This is due firstly to the fact that in Strategy 2, the degree of freedom is greater than in Strategy 1, and secondly to the fact that in Strategy 2, the functional models expressed as parameters of the wire improve the geometry of the network.

Table 4 shows, for each processing strategy, the horizontal 2D and 1D vertical reliability regions at a 95% and 5% confidence levels. For Strategy 2, it also indicates the percentage of improvement of the estimated standard deviation compared to Strategy 1.

If we focus on the 1/2 width of the horizontal 2D reliability region, we can see that using Strategy 2 instead of Strategy 1 decreases the length values by at least 25% for point P2 and up to 67% for point F5. For points P2, T5, F2 and F5, the observation linked with the 1/2 length of the reliability region is the same in both strategies. This can be seen in Table 4 by the fact that the orientation of the regions remain close to each others. The fact that small differences exist in the orientation values corresponds to small changes due to the functional models between strategies. The

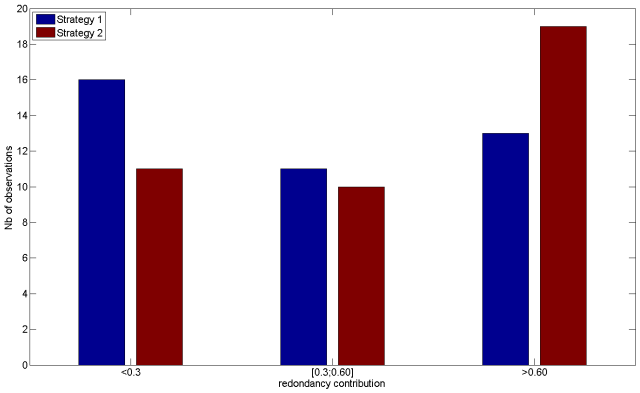

Figure 6: Distribution of redundancy contribution values for the observations in intervals $[0, 0.3[$, $[0.3, 0.60]$ and $]0.6, 1]$ for each strategy.

1/2 width of the 2D horizontal reliability region is also impacted by the strategy used: computed values in Strategy 2 are smallest than in Strategy 1, with percentage of improvement up to 77% for point F3. We can also notice the case of point F4 for which Strategy 1 gives a smallest value than Strategy 2. If we focus on the vertical reliability region, we can see that using Strategy 2 improves the length values, by at least 2% for point P2 and up to 72% for point F2. Thus, using Strategy 2 instead of Strategy 1 can really improve the reliability regions parameters.

CONCLUSION

In this contribution, we show that using basic stretched wire in a 3D longitudinal network can improve the geometry of the geodetic network, both in terms of accuracy and reliability. In our test network, conducted in a 5 m wide and 60 meters long network, with a polypropolen braided rope type, lightly tensed wire over 50 m, we show that one can expect accuracy improvements of about 3 to 47% along the radial axis of the network, but also along the longitudinal and vertical axes. We also show that using such a stretched wire can improve the redundancy contributions values of the observations, and the reliability regions (horizontal and vertical), with a percentage of improvement up to 70% in some cases.

A key problem in our practical methodology is the pointing accuracy on the marks located on the wire, and the fact that only angle measurements are performed on the wire. In future work, we will investigate these problems, and test several methods such as the use of small pearls on the wire to improve manual pointing accuracy, and to be able to perform distance measurements. We will also test different shapes for the 3D longitudinal network, by means of simulations and test campaigns, and will use stretched wires over more than 100 m.

Point	Strategy	1/2 Length (mm)	1/2 Width (mm)	Azim (deg)	Vertical (mm)
P2	1	13.2	0.5	133	0.5
	2	9.9 (25)	0.5 (0)	133	0.5 (2)
T5	1	14.9	0.5	133	0.5
	2	5.6 (62)	0.5 (0)	133	0.5 (4)
F1	1	28.7	15.3	33	1.6
	2	21.0 (27)	11.4 (25)	77	1.4 (15)
F2	1	16.8	9.6	53	1.9
	2	10.6 (37)	2.4 (75)	45	0.5 (72)
F3	1	18.2	14.1	87	1.7
	2	9.4 (48)	3.3 (77)	42	0.5 (70)
F4	1	15.1	2.7	138	1.1
	2	10.1 (33)	4.5 (-65)	44	0.5 (50)
F5	1	47.3	19.0	55	1.7
	2	15.5 (67)	8.2 (57)	54	1.4 (14)

Table 4: Horizontal and vertical reliability regions (at a 95% and 5% confidence levels) for each point of the network and for each processing strategy, in millimeters. In parenthesis, the percentage of improvement over Strategy 1.

REFERENCES

[1] J-P Quesnel, H. Mainaud-Durand, T. Touzé, Stretched wire offset measurements : 40 years of practice of this technique @ CERN for aligning the accelerators of particle, IWAA 2008, KEK, Japan, Feb. 2008

[2] D. Missiaen, T. Dobers, M. Jones, C. Podevin, J.P. Quesnel, The Final Alignment of the LHC, IWAA 2008, KEK, Japan, Feb. 2008

[3] H. Mainaud Durand, P. Bestmann, A. Herty, A. Marin, V. Rude, oWPS VERSUS cWPS, IWAA 2012, Fermilab, USA, Sep. 2012

[4] T. Touzé, Calcul des flèches de fils tendus depuis la mesure de leurs fréquences d'oscillation transversale, CERN Report EDMS 1108245, 2010

[5] M. Duquenne, S. Durand, V. Rude, H. Mainaud-Durand, T. Touzé, Improving 3D longitudinal network measurement by using stretched wire, IWAA 2016, ESRF, France, Oct 2016

[6] W.F. Caspary Concepts of network and deformation analysis. Edited by. J. M. Rueger. Third (corrected) Impression, 2000.

[7] P. E. Ciddor., Refractive index of air : new equations for the visible and near infrared. In: Optics and Photonics Journal, 35.9, pp. 1566-1573, March 1996.

[8] Stéphane Durand, CoMeT - Compensation de Mesures Topographiques, IDDN.FR.001.490017.000. R.P.2017.000.31235, 2017